Performance analysis of CKF algorithm for battery SoC estimation with its aging effect

G. Geetha Ravali, K. Narasimha Raju

Department of Electrical and Electronics Engineering, Koneru Lakshmaiah Education Foundation, Vaddeswaram, India

Article Info	ABSTRACT
	The penetration of electric vehicle (EV) in automobile market is very much dependent on the battery technology. Its size, weight, and cost are issues of concern. To effectively utilize the battery expertise, precise estimate of state of charge (SoC) is vital which greatly depends on the battery model. Current models lack consideration for variations in battery capacity over their lifespan. This paper develops a battery model which depicts the depletion of battery capacity with its life. Subsequently, this model has been utilized for estimation using advanced Kalman filtering (KF) algorithms. For the developed model, the design and effectiveness of the cubature Kalman filter (CKF) is applied as a proposed robust state-estimator for this problem. Moreover, a comparative analysis was undertaken with existing non-linear KFs based on performance metrics. The optimal choice of estimator is identified, through the results obtained from the Octave/MATLAB simulation. The outcomes show CKF algorithm based SoC estimator is superior to others in ensuring high accuracy, strong robustness even under changes in initial conditions (i.e., initial SoC, process and sensor noise levels), system's ability to converge quickly while ensuring that the maximum error in state of charge (SoC) estimation remains within 1% after convergence.

Corresponding Author:

K. Narasimha Raju
Department of Electrical and Electronics Engineering, Koneru Lakshmaiah Education Foundation
Vaddeswaram, Andhra Pradesh, India
Email: narasimharaju_eee@kluniversity.in

NOMENCLATURE

z	: State of charge	x[k+1]	: State prediction time update
v(t)	: Terminal voltage	Δt	: Sampling interval
i(t)	: Battery instant discharge current	i_{R1}	: Current through R_1 and C_1
η	: Coulombic-efficiency	$h[k]$	: Hysteresis
Q	: Capacity	γ	: Rate of decay
T	: Temperature	M	: Maximum plus/minus hysteresis
R	: Resistance	Sgn(z)	: Forces stability for both dis/charge
C	: Capacitance	A_{RC}, B_{RC}, A_H	: Arbitray constants
A[k]	: State transition matrix	R	: Gas constant
B[k]	: Control-input matrix	Z	: Adjustable factor
u[k]	: Control input	A	: Factor of pre-exponential term
E_a	: Activation energy	T	: Absolute temperature
N	: Cycles under discharge/charge	y_k	: Output equation
v_k	: Sensor noise	w_k	: Process noise
$\sum_{\tilde{x},k}^{+}$	: Error covariance estimate	μ	: Mean

1. INTRODUCTION

The development of electric vehicles (EVs) will mitigate contingent on fossil fuels for transportation. By using electricity, which can be generated from a variety of sources, countries can enrich their utility choices therefore mitigate its reliance on oil imports. Ultimately, the overarching goals include mitigating climate change, lowering the transportation sector's global emissions while progressing in the stride to a cleaner, greener future [1]. The development of EVs fosters technological innovation in various aspects, driving improvements in performance, range, efficiency, and user experience. Some notable areas of innovation include battery technology, energy storage, electric motors and drivetrain systems, range extension, vehicle-to-grid technology, autonomous driving integration, and charging infrastructure [2], [3]. The achievement of further advancements and widespread adoption of electric vehicles hinges significantly on the effectiveness of battery packs as the primary power source. In EV market, lithium-ion batteries are becoming ever more prevalent compared to others owing to their superior energy/power density, zero memory impact, deeper life expectancy, and extended cycling [4], [5]. Consequently, a critical aspect of enhancing modern EV performance is the crucial software component of battery management systems involves parameters (voltage, current and temperature) and states (state of charge (SoC), state of health (SoH), and state of power (SoP)) monitoring [6]. SoC acts as a key element and host for other operations and calculations, thus, precise SoC estimate maximizes battery consumption by providing accurate travel distance and ensures safe operating limits for the battery. SoC gives definite estimates in driving range and the leftover capacity within the pack that plays an energetic position in optimizing the charging and discharging processes control [7]. Direct measurement of SoC is not feasible since it is not a physical quantity. Therefore, SoC can only be reliably estimated. Even so, driven by the intense nonlinear properties and time-variance system of batteries, challenges persist to achieve precise assessments on SoC upon intricate real-world circumstances, compounded by other diverse influencing factors like fluctuating temperature range, and aging status [8].

Over the past decade, most research in the issue has emphasized the use of enhancing the accuracy of SoC estimation to offer a clear concept to the researchers and manufacturers for the imminent EV progression. Various SoC estimation techniques that are widely employed are voltage-based/look-up, current-based/coulomb-counting/ampere-hour integration, model-based, and data-driven techniques. In majority of the cases, researchers predominantly focused on model-based and data approaches [9], [10]. The traditional look-up table used the direct-mapping correlation between SoC and parameters describing exterior characteristics, such as impedance and open-circuit voltage. The relation was tabulated through thorough lab tests. In real-world applications, especially beyond controlled laboratory settings, lithium ion batteries (LIB) was typically operated continuously, hence not practical. In contrast, the coloumb counting (CC) was fairly accurate under known initial conditions, precise sensor calibration, and aging levels. Inaccuracies couldn't be avoided in this case because of its open-loop mechanism. Despite the simplicity of traditional methods (voltage, and current-based), the results realize the flaws of long resting time, unknown initial SoC, high accuracy measurement in voltage, and sensor error. This uncertain initial value creates an error of 20% more which can be reduced by effective error recalibration from the mapping relationship of SoC versus open circuit voltage (OCV) table as presented in [11], [12]. With known initial SoC, sensor calibration, and updated capacity, ampere-hour integration (AHI) attains accurate accuracy as stated in [13]. From the author's findings, it is observed that the combination of these methods may possibly give better accuracy but remains ubiquitous and inapplicable for online assessment. The idea of a combined approach is supported by studies [14], [15], which deliver efficient operation. Despite the fact, measuring the OCV in real-time proves challenging due to uncertain driving cycles, complex application circumstances, and other variables. Based on these findings, identifying a precise and straightforward model is a crucial concern, necessitating the widespread utilization of model-based methods (analytic and statistical/empirical linearization) like observers, and filtering techniques for accurate SoC estimation [16]-[18]. Another possibility would be data-driven approaches, that rely on the analysis and utilization of data for estimation process. Instead of relying solely on predefined models, these approaches use real-world data to make predictions and assess the status of a battery. From the experimental datasets, researchers employ meta-heuristic techniques, and machine learning or statistical methods to process and interpret the information obtained from the battery [19], [20]. They don't rely on a predefined model structure and can adjust to diverse and dynamic scenarios. Also, can learn directly from operational data, reducing the impact of modeling errors. But then, they come with inherent drawbacks like limited generalization, data dependency, absence of physical interpretability, overfitting, computational complexity, and robustness concerns.

To anticipate the internal dynamic behaviors of a battery, it is essential to create a model for the battery. Equivalent circuit models [21], characterized by their simple structures, offer a practical approach without requiring prior knowledge of electrochemistry as mentioned in [22]. However, these conventional models lack physical insights, and uncertainties like hysteresis and aging effect and, consequently, are not suitable for estimating the health-related states and power management. In comparison, models rooted in fundamental electrochemical and thermodynamic principles, commonly referred to as physics-based models like pseudo-two-dimensional as presented in [23], excel in providing more valuable and essential information.

They prove adept at predicting battery health and play a crucial role in the development of optimal control strategies [24]. But then implementing highly nonlinear partial differential-algebraic equations on battery management system (BMS) for online application is impractical due to computational complexity as mentioned in [25]. In light of these conclusions, there is a need for an enhanced circuit model of a lithium-ion battery that can address uncertainties, thereby making accurate estimation possible. Among the existing models, the absence of degradation dynamics, capacity estimation and adaptive estimation of unknown error covariance results in inaccuracy of the performance as mentioned in [26], [27]. For many years, this capacity degradation/ aging effect phenomenon was surprisingly neglected in the modelling and estimation process. The above finding is related to the study of [28] that the theory of Li-ion battery ageing results in capacity fade, and nonlinear ageing. These studies focus on developing a model that can predict lifetime prediction of cell capacity. Following this, forecasts both linear/nonlinear degradation based on varied constant current cycling data (C/3 charging - 4C discharging) (here C-Crate; a relative measure of current), demonstrating a 98% goodness-of-fit-error with surpassing the performance of established aging models. The result in [29]-[32] addressed certain challenges mentioned earlier, suggesting an enhanced battery model for SoC estimation and degraded-capacity through an improved extended Kalman filter (KF). A similar model is used by [33] with particle swarm optimization technique to mitigate the potential for prediction deviation, alongside fostering the process-noise covariance vector resulting from accumulated errors during prolonged operation.

In contrast, the study by [34] indicated that an improved adaptive extended Kalman filter can accomplish co-estimation for battery capacity and SoC and is proven, ensuring that the SoC error remains within ±1.2% during the initial 50 seconds, and the relative capacity error is restricted to within 2% after convergence. However, the study solely considered the hysteresis effect, and complexity of driving conditions and overlooked the potential challenges that the battery encounters during prolonged exposure to high C-rates and aging as shown by the studies in [35], [36]. On the other hand, a search of the literature revealed that limited studies have focused on machine learning (ML) techniques due to the complexity in model-based [37], [38]. Having said that in future, integration of model and data-driven methods can be an effective progression for further accuracy [39]. Authors in [40], [41] added that multi-state estimation plays a critical role in the enhancement of battery performance. Their methodology incorporates the application of an ensemble-empirical mode decomposition with adaptive noise, combined to an autoencoder considering model uncertainties. Updates on various parameters and time scales is accomplished through the dual-extended Kalman filter. For improving the rate of estimator, the study used the variable forgetting factor limited memory recursive least squares technique. Similarly, the authors in [42], [43] found that electrochemical impedance spectroscopy is also a powerful tool for achieving precise state estimation. Conversely, in real-world applications, the implementation of electrochemical impedance spectroscopy (EIS) may require specialized equipment, sophisticated analytical techniques, and careful control of experimental conditions. Alternatively, the study by [44] suggested an adaptive fractional-order square root unscented KF which dynamically updates disturbance statistics in real-time addressing the problem of deviation brought on by improper noise covariance matrices. In comparison to other KFs as mentioned above, the studies by [45], [46] suggest that cubature Kalman filter (CKF) excels in handling the complexities of nonlinear dynamics, providing more reliable, and precise estimates. Its adaptability and effectiveness make it a valuable tool for applications ranging from robotics and navigation systems to signal processing and control engineering.

Even though there has been quantitative analysis of various estimation techniques, no detailed investigation of model uncertainties (hysteresis), capacity estimation concerning the aging effect, which are the major challenges to be addressed for enhancement or of battery performance, and practicality. In regard to this, advancements should collectively aim to address these confronts correlated with the superior state estimation procedure, achieving more reliable and robust battery state estimation in various applications. Interestingly, previous research has not explored battery modeling with hysteresis and ageing effects in the estimation practice. In view of these shortcomings, CKF, as a robust state estimator, is proposed in this field of work. The key contribution of the article is as follows:

- A state-space representation of the battery model and mathematical model of capacity degradation or aging effect is made for the effective state estimation;
- As a state-of-art robust algorithm, the CKF method is developed to obtain better accuracy in SoC estimation under capacity degradation or aging effect; and
- Comparative analysis of the proposed CKF with other KFs under equivalent nonlinearities and aging effect.

The remaining paper is organized as follows. Section 2 first describes the complete battery model. Next, the detailed mechanism for aging is presented and its mathematical model has been developed for capacity estimation. Section 3 explains conventional and proposed SoC estimation methodologies with its algorithms. In section 4, the effectiveness of the proposed robust CKF technique is verified with comparison of other filtering techniques. Finally, section 5 provides a summary of the findings.

2.   BATTERY MODEL AND MODEL PARAMETERS IDENTIFICATION
2.1. Enhanced self-correcting model

Developing a concise and accurate battery model is the pre-requisite condition that significantly impacts the precision of the SoC estimation. Compared to various models available for Lithium-ion batteries, as discussed earlier concerning stability, nonlinearities, precision, and less complicated computing in SoC estimation, the enhanced self-correcting (ESC) model was developed, as depicted in Figure 1. The developed model incorporated parameters related to diffusion, OCV as a measure of SoC, and ohmic resistance, including the hysteresis effect. Hysteresis is a path-dependent voltage that does not decay to zero when the cell rests, unlike diffusion voltages that change with time. The model parameters were determined using experimental data from the 18650-battery cell. To determine the model parameter values, the functions were associated with a toolbox named ESC in Octave/MATLAB which provides access to the model fields (process OCV and process dynamic). Table 1 tabulates the battery specifications.

The discrete form of mathematical equations is written for the above model. In discrete time, the assumption was made that the current remains persistent within the entire interval. Each attribute of dynamic nature ensues within (1) and (2).

$$x[K + 1] = A[K]x[K] + B[K]u[K] \tag{1}$$

$$\begin{bmatrix} z[K+1] \\ i_{R1}[K+1] \\ h[K+1] \end{bmatrix} = \begin{bmatrix} 1 & 0 & 0 \\ 0 & A_{RC} & 0 \\ 0 & 0 & A_H[K] \end{bmatrix} \begin{bmatrix} z[K] \\ i_{R1}[K] \\ h[K] \end{bmatrix} + \begin{bmatrix} -\eta[K]\Delta t/Q & 0 \\ B_{RC} & 0 \\ 0 & A_H[K]-1 \end{bmatrix} \begin{bmatrix} i[K] \\ sgn(i[K]) \end{bmatrix} \tag{2}$$

Since SoC (the battery residual/leftover capacity) isn't a physical quantity. Therefore, SoC can be approximated utilizing the battery-measured values (voltage, current, and temperature).

$$SoC = \frac{Q_{available}}{Q_{rated}}; \; Z[k+1] = Z[k] - \frac{\Delta t}{Q} i[k] \tag{3}$$

Computing terminal voltage of the battery as (4) and (5).

$$y[K] = C[K]x[K] + D[K]u[K] \tag{4}$$

$$V[k] = OCV(z[K], T[K]) + M_0 S[K] + Mh[k] - R_1 i_{R1}[K] - R_0 i[K] \tag{5}$$

This mathematical model was subjected to integration with filtering algorithms for estimating the battery states.
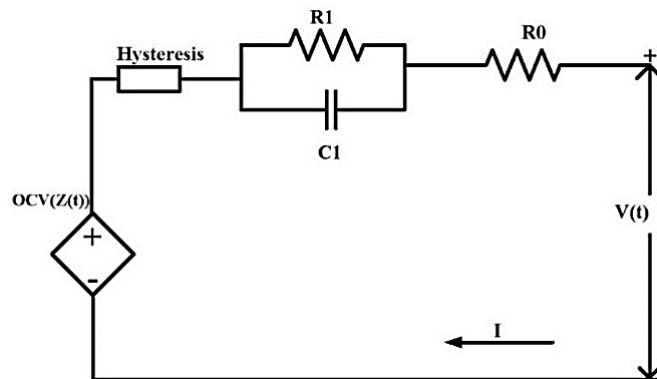

Figure 1. Battery model

Table 1. Battery cell particulars

Battery parameter	Specification
Type	LiNMC
Upper/lower cut-off voltage	4.2/2.5 V
Nominal voltage	3.6 V
Nominal capacity	25 Ah

2.2. Capacity degradation/aging model

Understanding and mitigating the effects of aging is crucial for optimizing battery lifespan and maintaining reliable performance. Apart from various aging mechanisms referred to [47] were tabulated in Table 2, temperature, C-rate, depth of discharge, SoC, were the central variables imperiling the development of aging. To demonstrate the impact of aging, the model was developed by incorporating the temperature and power-law relation. This combination provides a comprehensive approach, allowing us to understand temperature variations and the complex, non-linear nature. Thus, the model that incorporates the above factors helps account for the impact of aging on capacity. With this, the relative capacity was assessed, inferring the extent of aging and degradation that occurred.

The temperature dependence of reaction rates by Arrhenius equation can be of the form as (6).

$$K(T) = A \times \exp\left(\frac{-E_a}{RT}\right) \tag{6}$$

Here, k(T) is the reaction rate constant at temperature, A is the pre-exponential factor depends on current (assumed to be $1 \times 10-6$ nm/s for illustrative purposes), E_a is the activation energy for cycling aging (in J/mol or kJ/mol), R is the universal gas constant (8.314 J/mol\cdotpK), T is the absolute temperature in Kelvin.

For instance, the growth of the SEI layer can often be described by a power law of the form as (7).

$$SEI\ thickness = K(T) \times N^z \tag{7}$$

Here, SEI thickness is the thickness of the SEI layer (nanometers (nm) over time and cycle count), k(T) is the temperature-dependent rate constant from the Arrhenius equation, N is cycle count, z is the power law exponent. Capacity loss is calculated as (8).

$$Q_{initial} \times (1 - K(T) \times N^z) \tag{8}$$

The parameter values for capacity loss calculation are given in Table 3. The battery's capacity has diminished to around 20 ampere-hours (Ah) after 1000 cycles as shown in Figure 2.

Table 2. Aging mechanisms

Cause	Effect	Leads to	Enhanced by
Continuous low-rate electrolyte decomposition builds SEI	Li loss, impedance rise	Capacity/power fade	SoC, temperature rise
SEI growth leading to surface area reduction	impedance rise	Power fade	SoC, temperature rise
Changes in porosity due to volume change and SEI growth	impedance rise	Power fade	Increased SoC, cycling rate
Metallic Li plating, subsequent electrolyte decomposition	Lithium (electrolyte) loss	Capacity (power) fade	Low temperature, high charge rates
Graphite exfoliation, gas evolution, solvent co-intercalation	Active material failure, Li loss	Capacity fade	Overcharge
Contact b/w particles lost due to volume changes	Loss of active material	Capacity fade	High rate, low cell SOC
Decomposition of binder	Mechanical stability deficit, Li deficit	Capacity fade	SoC, temperature rise
Graphite exfoliation, gas evolution, solvent co-intercalation	Li loss, active material deficit	Capacity fade	Overcharge
Phase transitions	Cracking of active particles	Capacity fade	High rates, high/low SOC
Structural disordering	Li sites lost and Li trapped	Capacity fade	High rates, high/low SOC
Metal dissolution and/or electrolyte	Migration of soluble species	Capacity fade	High/low SOC, high temperature
Decomposition	Reprecipitation of new phases, form surface layer	Power fade	
Electrolyte decomposition	Gas evolution		High temperature
Binder decomposition, oxidation of conductive agent	Connectivity loss	Power fade	
Corrosion of current collector	Connectivity loss	Power fade	High SOC

Table 3. Parameter values for capacity degradation model

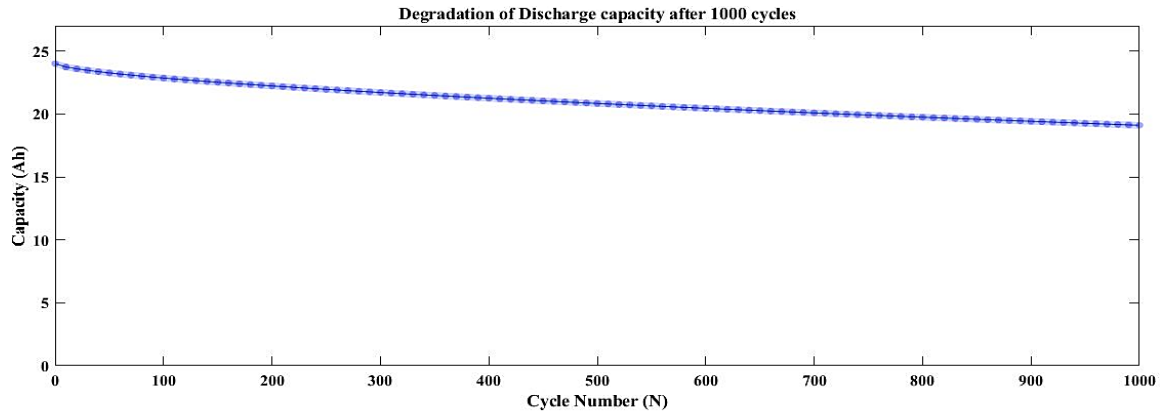| A	E_a/R	z
0.3687	1472	0.6405

Figure 2. Degradation in capacity observed in a Li-ion cell after undergoing 1000 cycles

3. METHODOLOGY

Every approach implements a different methodology to evaluate the SoC performance. Alternative to the conventional approaches discussed, KF makes it a top choice for real-time state estimation for its optimality, adaptability, efficiency, robustness, versatility, ability to handle sensor data, and well-established mathematical theory. KF is a special case of sequential probabilistic inference, yielding an optimal state estimate through the minimum mean-squared error approach. However, its reliance on a Gaussian distribution assumption posed challenges when confronted with non-Gaussian distributions, a common occurrence in real-world scenarios [48]. As batteries were subjected to non-linear characteristics, it was critical for models relating to them to also be of a non-linear nature. A non-linear relationship between the SoC and resultant voltage was observed in rechargeable batteries, rendering the entire propagation potentially incompatible with a Gaussian environment.

3.1. Non-linear KF techniques

Unlike linear Kalman filters, which were specifically designed for linear systems, non-linear Kalman filters, were more flexible and capable of accommodating non-linear relationships [49]. In the presence of non-linearities, these filters contributed to enhancing the performance and reliability of BMS. Different non-linear variants for state estimation were applied to the developed battery model with its aging affect.

3.1.1. Extended KF

Extended Kalman filter (EKF), an analytical linearization of the system model under every time instance. Similar to KF, EKF followed the same working principle but employed a linearization approach, operating through a two-step estimation process shown in Figure 3. Generalizing the nonlinear case with system dynamics:

$$x_k = f(x_{k-1}, u_{k-1}, w_{k-1}) \tag{9}$$

$$y_k = h(x_k, u_k, v_k) \tag{10}$$

estimator provides an output state estimate $\hat{x}_k^+$, error covariance estimate $\sum_{\tilde{x},k}^+$, however, exists high certainty that the true value falls within $\hat{x}_k^+ \pm 3\sqrt{\text{diag}(\sum_{\tilde{x},k}^+)}$ (bounds) and expecting until subsequent interval comes, updating k and proceeding to state prediction step. Hence, this demonstrates a recursive process.

3.1.2. Central difference KF

Central difference Kalman filter (CDKF), a statistical or empirical linearization of the system model for every time instance. Given an input random variable $x \in R^n$ and $x \sim (\mu, \sum)$, where μ or $\bar{x}$ or X_0 represents the mean and $\sum$ is the covariance, the generation of $p + 1 = 2n + 1$ (with n being the system dimension) sigma points entail the creation a matrix with a specified essential. Central difference transformation:

$$\bar{x} \text{ or } X_0 = \hat{X}(k|k) \tag{11}$$

$$\text{for i=1, ..., n} \qquad X_i(k|k) = (X_0 + \gamma\sqrt{\sum_{\bar{x}}})_i \tag{12}$$

$$\text{for i=n+1, ..., 2n} \qquad X_i(k|k) = (X_0 - \gamma\sqrt{\sum_{\bar{x}}})_{i-n} \tag{13}$$

where, $\widehat{X}(k|k)$ is a vector of length n for which the sigma points are computed, $\sum_{\tilde{x}}$ is its covariance matrix and w^m and w^c are weights associated with the sigma points for estimating the mean vectors and covariance matrices, respectively. $(\gamma\sqrt{\sum_{\tilde{x}}})_i$ is the ith column of the matrix square root, e.g., lower triangular Cholesky factorization.

Values in weights used by CDKF are (14)-(17).

$$\gamma = h \tag{14}$$

$$w_0^{(m)} = \frac{h^2 - n}{h^2} \tag{15}$$

$$w_0^{(c)} = \frac{h^2 - n}{h^2} \tag{16}$$

$$\text{for i=1, ..., n} \qquad w_i^{(c)} = w_i^{(m)} = \frac{1}{2h^2} \tag{17}$$

Thus, the ensemble of sigma points is produced as outlined (18).

$$\chi = \left\{ X_0, (X_0 + \gamma\sqrt{\sum_{\tilde{x}}}), (X_0 - \gamma\sqrt{\sum_{\tilde{x}}}) \right\} \tag{18}$$

$\widehat{X}(k|k)$ is computed from the sigma points generated, $\sum_{\tilde{x}}$ is covariance, and weights related to mean and covariance are w^m, w^c. $\sqrt{\sum_{\tilde{x}}}_i$ gives the factorization under the lower-triangular-Cholesky division. Here h=√3; tuning parameter.

Time Update ("Prediction")
- State prediction
$\hat{x}_k^- = E\left[f(x_{k-1}, u_{k-1}, w_{k-1}) | Y_{k-1} \right]$
- Error Covariance
$\sum_{\tilde{x},k}^- = E\left[f(x_k - \hat{x}_k^-)(x_k - \hat{x}_k^-)^T \right]$
- Predict system output
$\hat{y}_k = E\left[h(x_k, u_k, v_k) | Y_{k-1} \right]$

Measurement Update ("Correct")
- Kalman gain matrix
$L_k = \sum_{\hat{x}\hat{y},k} \sum_{\hat{y},k}^{-1}$
- State estimate
$\hat{x}_k^+ = \hat{x}_k^- + L_k(y_k - \hat{y}_k)$
- Error covariance
$\sum_{\tilde{x},k}^+ = \sum_{\tilde{x},k}^- - L_k \sum_{\tilde{y},k} L_k^T$

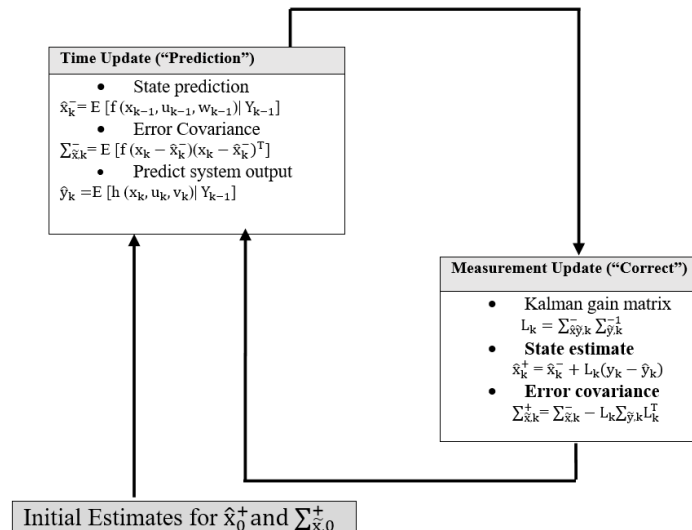Initial Estimates for $\hat{x}_0^+$ and $\sum_{\tilde{x},0}^+$

Figure 3. Implementation flowchart of KF, EKF algorithm

3.1.3. Unscented/Sigma point KF

Unscented Kalman filter (UKF)/sigma point Kalman filter (SPKF), a statistical linearization system. Sigma points (a deterministic sample points) were chosen to precisely estimate the statistics of the propagating method. Unscented transformation:

$$X_0 = \widehat{X}(k|k) \tag{19}$$

$$\text{for i=1, ..., n} \qquad X_i(k|k) = (X_0 + \gamma\sqrt{\sum_{\tilde{x}}})_i \tag{20}$$

$$\text{for i=n+1, ..., 2n} \qquad X_i(k|k) = (X_0 - \gamma\sqrt{\sum_{\tilde{x}}})_{i-n} \tag{21}$$

where, $\widehat{X}(k|k)$ is a vector of length n for which the sigma points are computed, $\sum_{\tilde{x}}$ is its covariance matrix and w^m and w^c are weights associated with the sigma points for estimating the mean vectors and covariance matrices, respectively. $(\sqrt{(n+\lambda)(\sum_{\tilde{x}})})_i$ is the ith column of the matrix square root, e.g., lower triangular Cholesky factorization.

Weight values for UKF/SPKF are (22)-(25).

$$\gamma = \sqrt{n + \lambda} \tag{22}$$

$$w_0^{(m)} = \frac{\lambda}{n+\lambda} \tag{23}$$

$$w_0^{(c)} = \frac{\lambda}{(n+\lambda)+(1-\alpha^2+\beta)} \tag{24}$$

for i=1, ..., n $\qquad\qquad w_i^{(c)} = w_i^{(m)} = \frac{1}{2(n+\lambda)}$ (25)

Where, $\lambda = \alpha^2(n + K) - n$, within the range of $(10^{-2} \le \alpha \le 1)$ and $k\epsilon\{0,3,-n\}$. In the given context, λ serves as the scaling parameter, k represents secondary scaling parameter, and to integrate preceding realization regarding the x propagation, β was employed. Additionally, α plays a crucial role in determining propagation around the mean x̄ (typically around 1e-3). In general, k and β were usually chosen as 0 and 2 respectively. The parameters for tuning the Gaussian probability density function were selected as follows: β=2, α=0.001, and k=0. Figure 4 illustrates the flow diagram of CDFK, UKF/SPKF algorithm. By incorporating the weights as $\{\gamma, w^{(m)}, w^{(c)}\}$; $w^{(m)}, w^{(c)}$ possess real scalar quantities, weighted moments were computed as (26) and (27).

$$X_0 = \sum_{i=0}^{2n} w_i^{(m)} \chi_i \tag{26}$$

$$\text{and } \sum_{\tilde{x}} = \sum_{i=0}^{2n} w_i^{(c)} (\chi_i - \bar{x})(\chi_i - \bar{x})^T \tag{27}$$

Followed by the propagation over sigma points through the function of nonlinearity, wherein transformed set of sigma points as $\mathcal{Y}$ is obtained. Then, computing output first statistical moments of $\mathcal{Y}$ transformed points as stated:

$$\mathcal{Y}_i = f(\chi_i) \tag{28}$$

$$Y_0 = \sum_{i=0}^{2n} w_i^{(m)} \mathcal{Y}_i \tag{29}$$

$$\text{and } \sum_{\tilde{x}} = \sum_{i=0}^{2n} w_i^{(c)} (\mathcal{Y}_i - \bar{y})(\mathcal{Y}_i - \bar{y})^T \tag{30}$$

Some of the theoretical differences in the functional process of NKFs were summarized in Table 4. Despite limitations, EKF was sensitive to the choice of initial conditions, and incorrect initialization or poor observability could lead to convergence issues, potentially diverging or converging to a local minimum. In contrast, UKF's effectiveness relied on the proper placement of sigma points, and as the state dimension increased, the growing number of sigma points could impact efficiency. Although UKF avoided EKF's linearization errors, the choice of sigma points introduced approximation errors, leading to inaccuracies in certain scenarios. Consequently, the aim was to address some of the limitations associated with other advanced NKF. Thus, proposed cubature KF as a robust estimator for SoC estimation.

3.1.4. Cubature KF: proposed robust state-estimator
CKF, a Bayesian filtering algorithm designed for nonlinear systems. CKF employed a cubature rule, instead of linearization, for accurate propagation of the system's covariance. The computational burden associated with CKF was comparatively lighter since it employed only 2n cubature points (where n is the system dimension), while UKF utilized 2n+1 sigma points for state and covariance propagation. Cubature transformation:

for i=1, ..., n $\qquad\qquad X_i(k|k) = (X_0 + \gamma\sqrt{\sum_{\tilde{x}}})_i$ (31)

for i=n+1, ..., 2n $\qquad\qquad X_i(k|k) = (X_0 - \gamma\sqrt{\sum_{\tilde{x}}})_{i-n}$ (32)

for i=1, ..., n $\qquad\qquad w_i = \frac{1}{2n}$ (33)

In this context, Q(k) and R(k) represented the matrices of covariance for process and sensor noises, respectively. Utilizing the weighted estimated covariance matrix, both UKF and CKF conversions generated sample indicates. Notably, for CKF, all points, including the center point, were assigned equal weight, resulting in a total of 2n points used. This uniform weighting simplified the sigma points and covariance calculations in CKF, ensuring a consistent treatment across all points. CKF does not involve as many tuning parameters as UKF. The selection of cubature points is often straightforward, making CKF a more parameter-free alternative,

simplifying the implementation, and reducing the need for parameter tuning. Figure 5 gives the flow diagram of CKF algorithm.
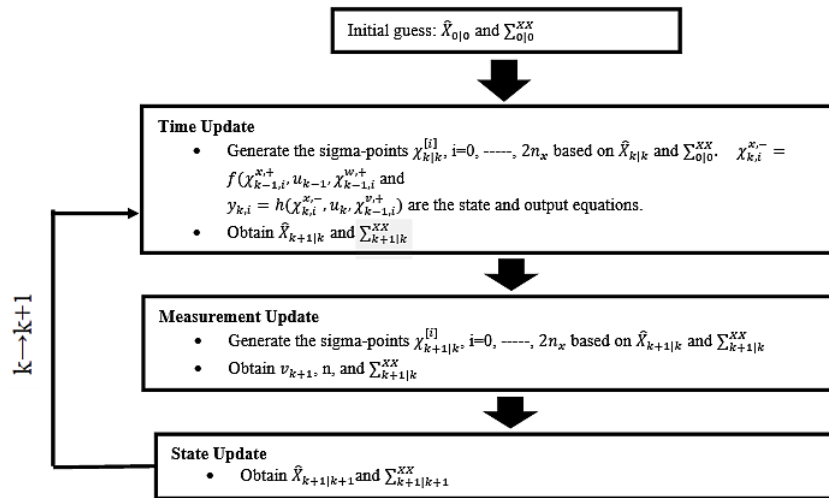

Figure 4. Flow diagram of CDKF and UKF/SPKF algorithm

Table 4. Theoretical comparison of non-linear KFs for estimating SoC

| System	Applicability	Assumptions	Limitations	Computational Complexity	Rate of estimate
EKF	Moderate nonlinear systems, Gaussian	Taylor-series expansion to linearize system equations for covariances	Linearizes the system at each step, may lead to inaccuracies in highly nonlinear systems	Moderate	High
CDKF/ UKF/ SPKF	Highly nonlinear systems, Gaussian	2n+1 sigma points, avoids linearization using carefully chosen sigma points	Requires tuning of scaling parameters, increased computational complexity compared to EKF	Moderate to high	High
CKF	Highly nonlinear, non-gaussian	2n cubature points, utilizes deterministic cubature sampling technique	Can be computationally intensive, especially in high-dimensional state spaces	High	Very high
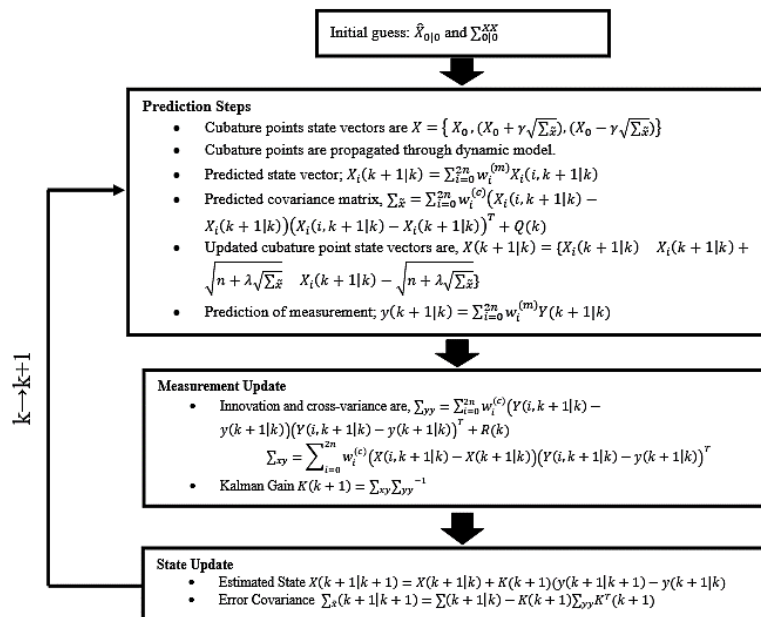
Figure 5. Flow diagram of CKF algorithm

4.   RESULTS AND DISCUSSIONS

Using the developed battery model including aging effect, these filtering techniques are implemented and simulated in Octave/MATLAB software. Based on the metrics: root mean square error, mean absolute error, and maximum error, the performance is assessed. Let N be the number of observations, $\hat{v}[k]$ be the estimated battery state, and $v[k]$ be the true (actual) battery state.

Root mean square error (RMSE) is a measure of the average magnitude of the errors between predicted values and actual values in a dataset.

$$\text{RMS} = \sqrt{\frac{1}{N}\sum_{j=1}^{N}(v[k] - \hat{v}[k])^2} \tag{34}$$

Maximum error (MAX) represents the maximum deviation or difference between predicted values and actual values in a dataset.

$$\text{MAE} = \frac{1}{N}\sum_{j=1}^{N}|v[k] - \hat{v}[k]|, \text{ and} \tag{35}$$

Mean absolute error (MAE) is a measure of the average magnitude of the errors between predicted values and actual values in a dataset. Unlike RMSE, MAE does not square the errors, making it less sensitive to outliers.

$$\text{MAX} = \max |v[k] - \hat{v}[k]| \tag{36}$$

Figures 6 and 7 indicate the estimation analysis for extended EKF and CDKF algorithms. The representation includes a black solid line denoting the estimate, a green solid line illustrating the true SoC versus time, and red lines indicating the SoC bounds. The calculation of error versus time involves determining the difference between the true value and the estimate, considering its bounds. To maintain a fair comparison, an identical random input is applied to both filters. EKF and CDKF algorithms' results indicate that errors surpass the bounds in EKF (RMSE: 0.42308%) but stay within bounds in CDKF (RMSE: 0.51543%) for the executed iterations.

Figure 8 indicates the estimation analysis for UKF/SPKF algorithm. Upon examination of the visualization, a clear understanding of the error magnitude in comparison to the true SoC emerges with RMSE of 0.57199%, highlighting the effective performance of the SPKF. Due to the increased number of sigma points, a computational burden occurred, along with tuning challenges for the parameters, making the filter less efficient.
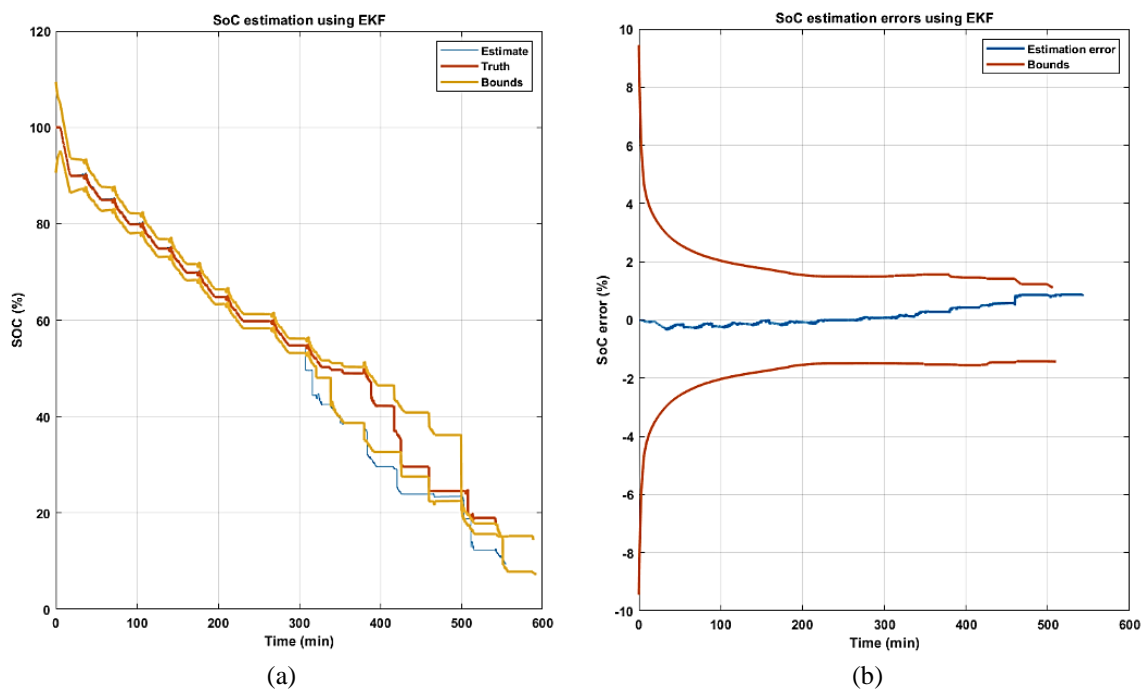

(a)   (b)

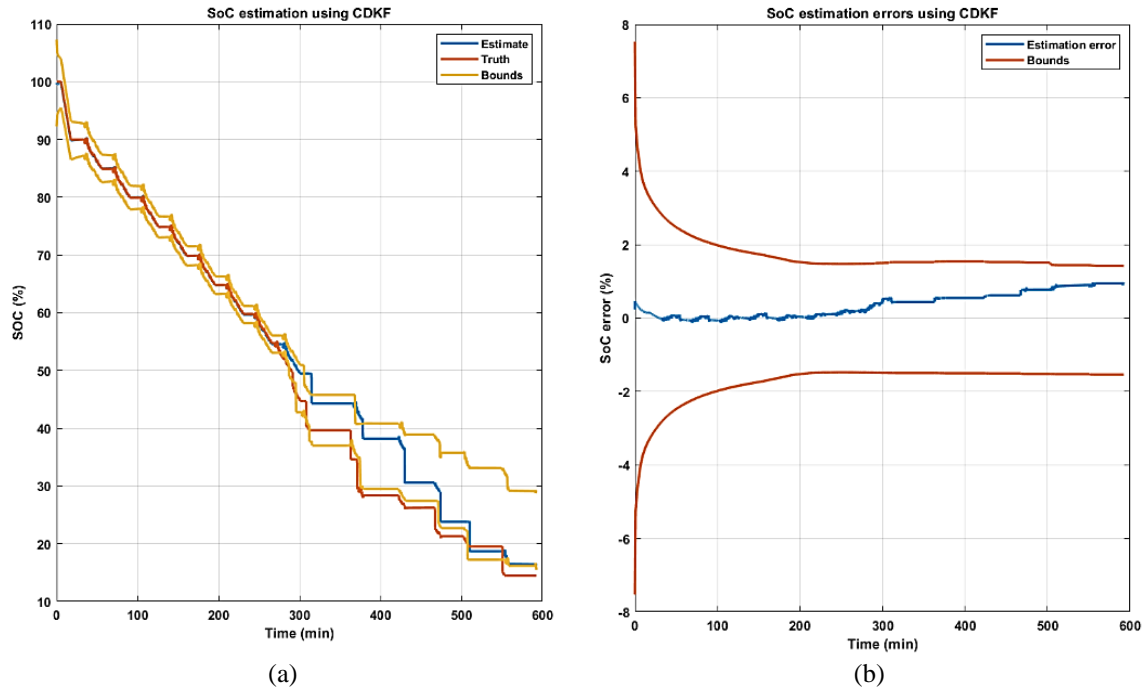Figure 6. EKF algorithm results for (a) SoC estimation and (b) SoC estimation error

(a)   (b)

Figure 7. CDKF algorithm results for (a) SoC estimation and (b) SoC estimation error

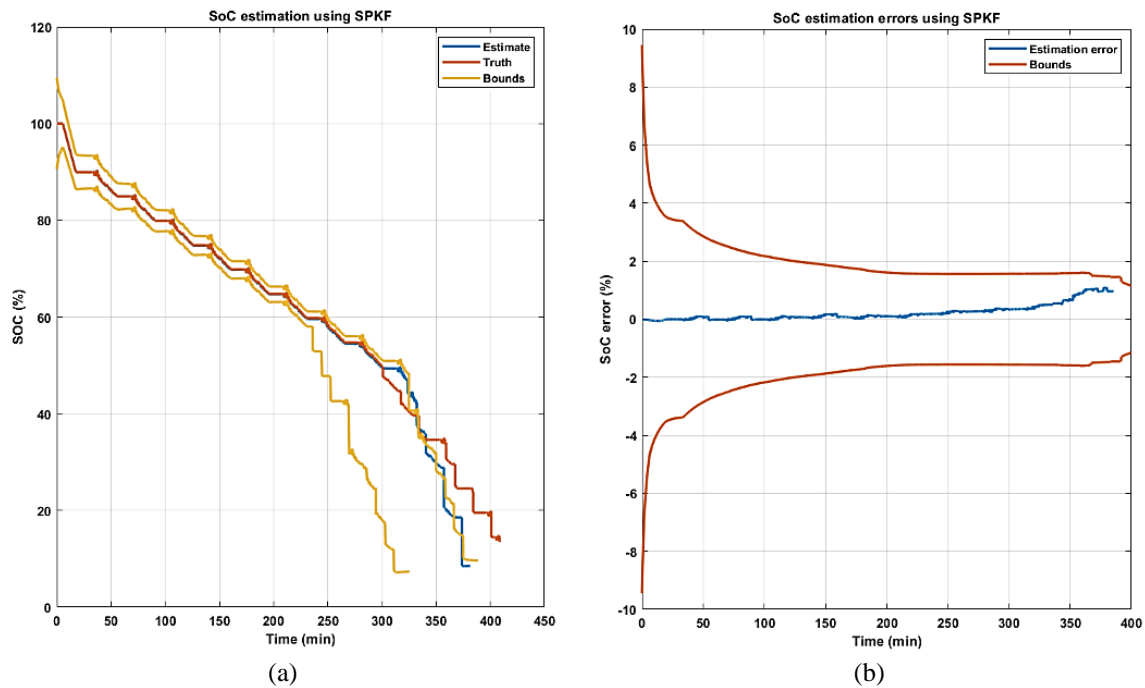(a)   (b)

Figure 8. UKF/SPKF algorithm results for (a) SoC estimation and (b) SoC estimation error

Figure 9 indicates the estimation analysis for CKF algorithm. This is a significant improvement compared to other filters under non-Gaussian noises and uncertainties with less computational complexity. The achievable RMSE is 0.49553%. In a practical system, the error constantly remains within the expected ranges and seldom approaches 0, due to the continuous influence of process noise on the actual system and the persistent presence of additive sensor noise in the measurements. Thus, errors stay within bounds, ensuring correct operation.

Table 5 lists the statistical comparison of non-linear KF estimators. This thorough comparison establishes the superiority of the CKF as a proposed robust estimator in SoC estimation, particularly in addressing high-dimensional nonlinear filtering challenges. Moreover, CKF exhibits operational proficiency in handling uncertainties related to modeling, initialization, and persistent noise (covariance). The suggested CKF approach functions well in real-time applications owing to processing power is a constant concern.
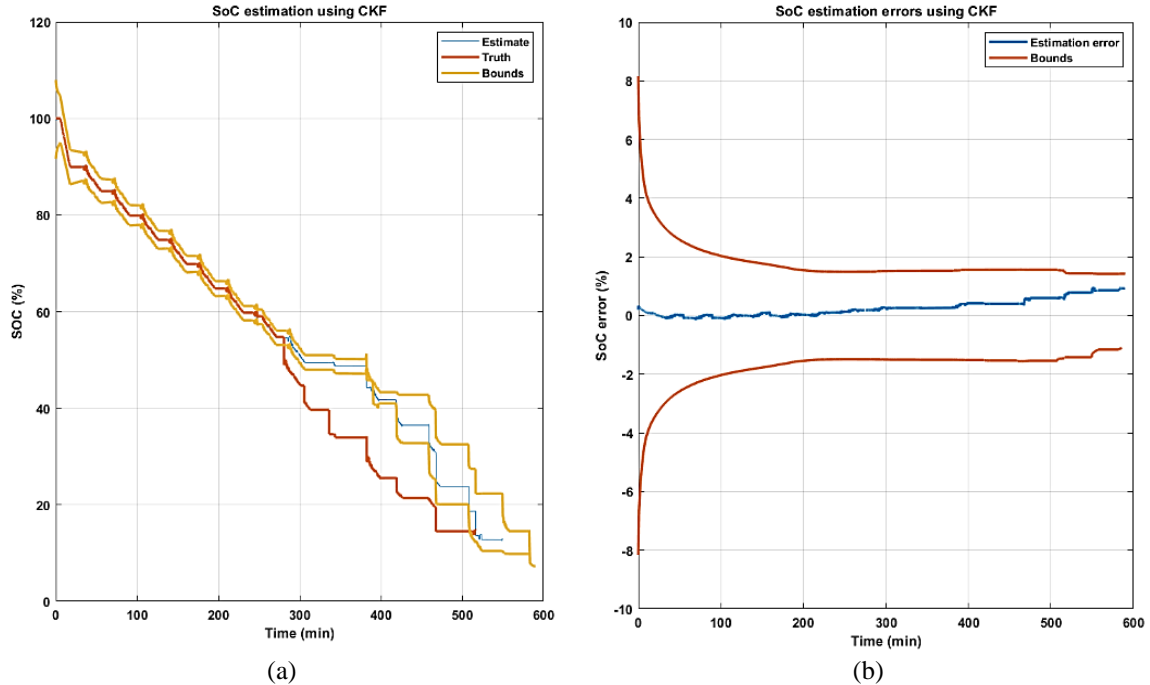
Figure 9. CKF algorithm results for (a) SoC estimation and (b) SoC estimation error

Table 5. Statistical comparison of non-linear KF state estimators

Filtering method	RMSE of SoC (%)	MAE (%)	MAX (%)
EKF	0.42308	0.32789	0.89901
CDKF	0.49298	0.36951	1.0029
UKF/SPKF	0.57199	0.43713	1.1293
CKF	0.49553	0.36870	1.0125

5. CONCLUSION

In this study, the goal was to develop an enhanced Li-ion battery model with an aging effect and assess the CKF's effectiveness as a robust Kalman filter variant for precise state estimation. This research has identified certain notable uncertainties, such as hysteresis and degradation/aging effect, which impact the battery characteristics and their performance in the practice of battery modelling and state estimation. Alongside the enhanced model with uncertainties, the study has gone some way towards enhancing our understanding of aging behaviour by generalizing with respect to temperature, cycle count, and combinations of stress factors. The simulation results from this study indicate that the modelled battery cell experiences capacity loss after 1000 cycles. Additionally, the findings from the filtering algorithms suggest that CKF quickly converges, reaching an RMSE of 0.49% across all uncertainties, showcasing its robustness and adaptability. The comparative results assist our understanding that CKF is superior and outperforms other non-linear KF under non-Gaussian and highly nonlinear systems. Further research might explore alternative degradation dynamics, concurrent estimation of both SoC and SoH, integration with cutting-edge models, and the development of non-intrusive or sensor less SoC estimation methods using CKF. These proposed areas hold significant potential in enhancing driving range accuracy, optimizing performance, ensuring safety, and achieving cost savings. Accordingly, they pave the way for more efficient and dependable battery management in the EV industry.

REFERENCES

[1]   G. Mittal, A. Garg, and K. Pareek, "A review of the technologies, challenges and policies implications of electric vehicles and their future development in India," *Energy Storage*, vol. 6, no. 1, p. e562, 2024, doi: 10.1002/est2.562.
[2]   D. Yadeo *et al.*, "Current trends in electric vehicle – Review," in *AIP Conference Proceedings*, Jun. 2024, doi: 10.1063/5.0202038.

[3]   P. Sharma, S. R. Salkuti, and S. C. Kim, "Advancements in energy storage technologies for smart grid development," *International Journal of Electrical and Computer Engineering*, vol. 12, no. 4, pp. 3421–3429, 2022, doi: 10.11591/ijece.v12i4.pp3421-3429.

[4]   M. N. Akram and W. Abdul-Kader, "Sustainable Development Goals and End-of-Life Electric Vehicle Battery: Literature Review," *Batteries*, vol. 9, no. 7, 2023, doi: 10.3390/batteries9070353.

[5]   S. R. Salkuti, "Advanced Technologies for Energy Storage and Electric Vehicles," *Energies*, vol. 16, no. 5, 2023, doi: 10.3390/en16052312.

[6]   M. Waseem, M. Ahmad, A. Parveen, and M. Suhaib, "Battery technologies and functionality of battery management system for EVs: Current status, key challenges, and future prospectives," *Journal of Power Sources*, vol. 580, 2023, doi: 10.1016/j.jpowsour.2023.233349.

[7]   H. J. Nanjappa and S. Channaiah, "Design and development of dual mode on-board battery charger for electric vehicle," *International Journal of Applied Power Engineering*, vol. 12, no. 2, pp. 153–161, 2023, doi: 10.11591/ijape.v12.i2.pp153-161.

[8]   L. Zhou *et al.*, "State Estimation Models of Lithium-Ion Batteries for Battery Management System: Status, Challenges, and Future Trends," *Batteries*, vol. 9, no. 2, 2023, doi: 10.3390/batteries9020131.

[9]   G. Jagadeesh, B. Arundhati, and K. Ravindra, "A review on modeling and estimation of state of charge of lithium-ion battery," *Advanced Technologies in Electric Vehicles: Challenges and Future Research Developments*, pp. 83–104, 2024, doi: 10.1016/B978-0-443-18999-9.00023-5.

[10]   P. Dini, A. Colicelli, and S. Saponara, "Review on Modeling and SOC/SOH Estimation of Batteries for Automotive Applications," *Batteries*, vol. 10, no. 1, 2024, doi: 10.3390/batteries10010034.

[11]   M. Tekin and M. İ. Karamangil, "Comparative analysis of equivalent circuit battery models for electric vehicle battery management systems," *Journal of Energy Storage*, vol. 86, 2024, doi: 10.1016/j.est.2024.111327.

[12]   W. E. Chang and C. C. Kung, "An Improved AhI Method With Deep Learning Networks for State of Charge Estimation of Lithium-Ion Battery," *IEEE Access*, vol. 12, pp. 55465–55473, 2024, doi: 10.1109/ACCESS.2024.3389969.

[13]   S. Das, S. Samanta, and S. Gupta, "Online state-of-charge estimation by modified Coulomb counting method based on the estimated parameters of lithium-ion battery," *International Journal of Circuit Theory and Applications*, vol. 52, no. 2, pp. 749–768, 2024, doi: 10.1002/cta.3806.

[14]   M. Karthikeyan, M. Nivas, H. Umesh Prabhu, and M. Ramesh Babu, "Improved State-Of-Charge Estimation Algorithms for Lithium-ion Batteries in Electric Vehicles," in *2024 Third International Conference on Intelligent Techniques in Control, Optimization and Signal Processing (INCOS)*, 2024, pp. 1-8, doi: 10.1109/INCOS59338.2024.10527653.

[15]   M. R. Ramezani-al and M. Moodi, "A novel combined online method for SOC estimation of a Li-Ion battery with practical and industrial considerations," *Journal of Energy Storage*, vol. 67, p. 107605, Sep. 2023, doi: 10.1016/j.est.2023.107605.

[16]   M. Zhou *et al.*, "Fractional-Order Sliding-Mode Observers for the Estimation of State-of-Charge and State-of-Health of Lithium Batteries," *Batteries*, vol. 9, no. 4, p. 213, 2023, doi: 10.3390/batteries9040213.

[17]   C. Li and G. W. Kim, "Improved State-of-Charge Estimation of Lithium-Ion Battery for Electric Vehicles Using Parameter Estimation and Multi-Innovation Adaptive Robust Unscented Kalman Filter," *Energies*, vol. 17, no. 1, p. 272, 2024, doi: 10.3390/en17010272.

[18]   N. K. Trung and N. T. Diep, "Coupling coefficient observer based on Kalman filter for dynamic wireless charging systems," *International Journal of Power Electronics and Drive Systems*, vol. 14, no. 1, pp. 337–347, 2023, doi: 10.11591/ijpeds.v14.i1.pp337-347.

[19]   F. Zhao, Y. Guo, and B. Chen, "A Review of Lithium-Ion Battery State of Charge Estimation Methods Based on Machine Learning," *World Electric Vehicle Journal*, vol. 15, no. 4, p. 131, 2024, doi: 10.3390/wevj15040131.

[20]   M. H. Zafar *et al.*, "Hybrid deep learning model for efficient state of charge estimation of Li-ion batteries in electric vehicles," *Energy*, vol. 282, p. 128317, 2023, doi: 10.1016/j.energy.2023.128317.

[21]   H. Nunes, J. Martinho, J. Fermeiro, J. Pombo, S. Mariano, and M. Do Rosario Calado, "Impedance Analysis and Parameter Estimation of Lithium-Ion Batteries Using the EIS Technique," *IEEE Transactions on Industry Applications*, vol. 60, no. 3, pp. 5048–5060, 2024, doi: 10.1109/TIA.2024.3365451.

[22]   A. M. AbdelAty, M. E. Fouda, A. S. Elwakil, and A. G. Radwan, "Fractional-Order Equivalent-Circuit Model Identification of Commercial Lithium-Ion Batteries," *Journal of The Electrochemical Society*, vol. 171, no. 5, p. 050553, 2024, doi: 10.1149/1945-7111/ad4a09.

[23]   J. Piruzjam, G. Liu, L. Rubacek, M. Frey, and T. Carraro, "On the analytical solution of single particle models and semi-analytical solution of P2D model for lithium-ion batteries," *Electrochimica Acta*, vol. 492, p. 144259, 2024, doi: 10.1016/j.electacta.2024.144259.

[24]   T. Wickramanayake, M. Javadipour, and K. Mehran, "A Novel Solver for an Electrochemical–Thermal Ageing Model of a Lithium-Ion Battery," *Batteries*, vol. 10, no. 4, p. 126, 2024, doi: 10.3390/batteries10040126.

[25]   A. Graule, F. F. Oehler, J. Schmitt, J. Li, and A. Jossen, "Development and Evaluation of a Physicochemical Equivalent Circuit Model for Lithium-Ion Batteries," *Journal of The Electrochemical Society*, vol. 171, no. 2, p. 020503, 2024, doi: 10.1149/1945-7111/ad1ec7.

[26]   J. Schmitt, M. Rehm, A. Karger, and A. Jossen, "Capacity and degradation mode estimation for lithium-ion batteries based on partial charging curves at different current rates," *Journal of Energy Storage*, vol. 59, p. 106517, 2023, doi: 10.1016/j.est.2022.106517.

[27]   X. Zhang, L. Duan, Q. Gong, Y. Wang, and H. Song, "State of charge estimation for lithium-ion battery based on adaptive extended Kalman filter with improved residual covariance matrix estimator," *Journal of Power Sources*, vol. 589, p. 233758, 2024, doi: 10.1016/j.jpowsour.2023.233758.

[28]   N. Kirkaldy, M. A. Samieian, G. J. Offer, M. Marinescu, and Y. Patel, "Lithium-ion battery degradation: Comprehensive cycle ageing data and analysis for commercial 21700 cells," *Journal of Power Sources*, vol. 603, p. 234185, 2024, doi: 10.1016/j.jpowsour.2024.234185.

[29]   R. M. Imran, Q. Li, and F. M. F. Flaih, "An Enhanced Lithium-Ion Battery Model for Estimating the State of Charge and Degraded Capacity Using an Optimized Extended Kalman Filter," *IEEE Access*, vol. 8, pp. 208322–208336, 2020, doi: 10.1109/ACCESS.2020.3038477.

[30]   A. S. Ogundana, P. K. Terala, M. Y. Amarasinghe, X. Xiang, and S. Y. Foo, "Electric Vehicle Battery State of Charge Estimation with an Ensemble Algorithm Using Central Difference Kalman Filter (CDKF) and Non-Linear Autoregressive with Exogenous Input (NARX)," *IEEE Access*, vol. 12, pp. 33705–33719, 2024, doi: 10.1109/ACCESS.2024.3371883.

[31]   Z. Liu, Z. Zhao, Y. Qiu, B. Jing, C. Yang, and H. Wu, "Enhanced state of charge estimation for Li-ion batteries through adaptive maximum correntropy Kalman filter with open circuit voltage correction," *Energy*, vol. 283, p. 128738, 2023, doi: 10.1016/j.energy.2023.128738.

[32]   K. Omiloli, A. Awelewa, I. Samuel, O. Obiazi, and J. Katende, "State of charge estimation based on a modified extended Kalman filter," *International Journal of Electrical and Computer Engineering*, vol. 13, no. 5, pp. 5054–5065, 2023, doi: 10.11591/ijece.v13i5.pp5054-5065.

[33]   V. A. Kusuma, A. A. Firdaus, S. S. Suprapto, D. F. U. Putra, Y. Prasetyo, and F. Filliana, "Leveraging PSO algorithms to achieve optimal stand-alone microgrid performance with a focus on battery lifetime," *International Journal of Applied Power Engineering*, vol. 12, no. 3, pp. 293–299, 2023, doi: 10.11591/ijape.v12.i3.pp293-299.

[34]   P. Nian, Z. Shuzhi, and Z. Xiongwen, "Co-estimation for capacity and state of charge for lithium-ion batteries using improved adaptive extended Kalman filter," *Journal of Energy Storage*, vol. 40, p. 102559, 2021, doi: 10.1016/j.est.2021.102559.

[35]   M. Bozorgchenani, G. Kucinskis, M. Wohlfahrt-Mehrens, and T. Waldmann, "Experimental Confirmation of C-Rate Dependent Minima Shifts in Arrhenius Plots of Li-Ion Battery Aging," *Journal of The Electrochemical Society*, vol. 169, no. 3, p. 030509, 2022, doi: 10.1149/1945-7111/ac580d.

[36]   S. Chen, Q. Zhang, F. Wang, D. Wang, and Z. He, "An electrochemical-thermal-aging effects coupled model for lithium-ion batteries performance simulation and state of health estimation," *Applied Thermal Engineering*, vol. 239, p. 122128, 2024, doi: 10.1016/j.applthermaleng.2023.122128.

[37]   A. Manoharan, K. M. Begam, V. R. Aparow, and D. Sooriamoorthy, "Artificial Neural Networks, Gradient Boosting and Support Vector Machines for electric vehicle battery state estimation: A review," *Journal of Energy Storage*, vol. 55, p. 105384, 2022, doi: 10.1016/j.est.2022.105384.

[38]   S. Singh, Y. E. Ebongue, S. Rezaei, and K. P. Birke, "Hybrid Modeling of Lithium-Ion Battery: Physics-Informed Neural Network for Battery State Estimation," *Batteries*, vol. 9, no. 6, p. 301, 2023, doi: 10.3390/batteries9060301.

[39]   T. E. Fan, S. M. Liu, X. Tang, and B. Qu, "Simultaneously estimating two battery states by combining a long short-term memory network with an adaptive unscented Kalman filter," *Journal of Energy Storage*, vol. 50, p. 104553, 2022, doi: 10.1016/j.est.2022.104553.

[40]   P. Takyi-Aninakwa, S. Wang, H. Zhang, Y. Xiao, and C. Fernandez, "Enhanced multi-state estimation methods for lithium-ion batteries considering temperature uncertainties," *Journal of Energy Storage*, vol. 66, p. 107495, 2023, doi: 10.1016/j.est.2023.107495.

[41]   C. Wang, S. Wang, J. Zhou, J. Qiao, X. Yang, and Y. Xie, "A novel back propagation neural network-dual extended Kalman filter method for state-of-charge and state-of-health co-estimation of lithium-ion batteries based on limited memory least square algorithm," *Journal of Energy Storage*, vol. 59, p. 106563, 2023, doi: 10.1016/j.est.2022.106563.

[42]   Y. Liu, L. Wang, D. Li, and K. Wang, "State-of-health estimation of lithium-ion batteries based on electrochemical impedance spectroscopy: a review," *Protection and Control of Modern Power Systems*, vol. 8, no. 1, p. 41, Dec. 2023, doi: 10.1186/s41601-023-00314-w.

[43]   X. Sun, Y. Zhang, Y. Zhang, L. Wang, and K. Wang, "Summary of Health-State Estimation of Lithium-Ion Batteries Based on Electrochemical Impedance Spectroscopy," *Energies*, vol. 16, no. 15, 2023, doi: 10.3390/en16155682.

[44]   R. P. Priya, S. R, and R. Sakile, "State of charge estimation of lithium-ion battery based on extended Kalman filter and unscented Kalman filter techniques," *Energy Storage*, vol. 5, no. 3, p. e408, Apr. 2023, doi: 10.1002/est2.408.

[45]   L. Chen, W. Yu, G. Cheng, and J. Wang, "State-of-charge estimation of lithium-ion batteries based on fractional-order modeling and adaptive square-root cubature Kalman filter," *Energy*, vol. 271, p. 127007, 2023, doi: 10.1016/j.energy.2023.127007.

[46]   J. Zhou, S. Wang, W. Cao, Y. Xie, and C. Fernandez, "Improved Backward Smoothing Square Root Cubature Kalman Filtering and Fractional Order—Battery Equivalent Modeling for Adaptive State of Charge Estimation of Lithium-Ion Batteries in Electric Vehicles," *Energy Technology*, vol. 11, no. 12, p. 2300765, 2023, doi: 10.1002/ente.202300765.

[47]   J. Zeng and S. Liu, "Research on aging mechanism and state of health prediction in lithium batteries," *Journal of Energy Storage*, vol. 72, p. 108274, Nov. 2023, doi: 10.1016/j.est.2023.108274.

[48]   C. Wu, W. Hu, J. Meng, X. Xu, X. Huang, and L. Cai, "State-of-charge estimation of lithium-ion batteries based on MCC-AEKF in non-Gaussian noise environment," *Energy*, vol. 274, p. 127316, Jul. 2023, doi: 10.1016/j.energy.2023.127316.

[49]   M. Khodarahmi and V. Maihami, "A Review on Kalman Filter Models," *Archives of Computational Methods in Engineering*, vol. 30, no. 1, pp. 727–747, 2023, doi: 10.1007/s11831-022-09815-7.

BIOGRAPHIES OF AUTHORS

G. Geetha Ravali 🆔 🇬 SC ◐ is a research scholar in the Department of Electrical and Electronics Engineering, Koneru Lakshmaiah Education Foundation, Vaddeswaram, Andhra Pradesh, India. She received B.Tech. degree in electrical and electronics engineering from Vignan Institute of Information and Technology, Duvvada, affiliated to JNTUK, Andhra Pradesh, India in June 2016, and masters (M.Tech.) in power systems and automation from GITAM Deemed to be University, Visakhapatnam, India in May 2018. Her research interests include battery energy storage systems, battery management systems, electric and hybrid vehicles, and estimation theory. She can be contacted at email: 183060021@kluniversity.in.

Dr. K. Narasimha Raju 🆔 🇬 SC ◐ has done his B.Tech. from Sri Venkateswara Hindu College of Engineering, Machlipatnam in electrical and electronics engineering in 2002, M.Tech. in power electronics and industrial drives from JNTUH in 2012 and Ph.D. from KLEF Deemed University in 2018. He has 20 years of teaching experience. Presently working as professor of EEE Department in KLEF. He was the former head of the department. He has published 31 Scopus-indexed journals and presented papers in 10 international conferences including, TENCON 2015 at Macau China. His research interests include PWM techniques for switched mode converters, novel multilevel inverter topologies, DC-microgrid, and algorithms for the determination of SOC, SOH, and SOL for energy storage devices used in electric vehicles and power systems. He also acts as the director of Centre for Innovation Incubation and Entrepreneurship (CIIE) and head of the Design Thinking and Innovation Department, KLEF Deemed to be University as a part of which he enables the academics to aid the innovative ideas of the students and transform them to start-ups. Presently he is guiding 4 research scholars and 4 scholars have successfully completed Ph.D. under his supervision. He has been presented with Uttam Acharya Award for the year 2019 by Indian servers and received the best teacher award for academic years 2012-13 and 2016-17 at KLEF. He can be contacted at email: narasimharaju_eee@kluniversity.in.